Manuscript ID: ASC2022-2LPo1L-08

Parametric Studies of the EU DEMO Central Solenoid

X. Sarasola, P. Bruzzone, K. Sedlak, V. Corato, L. Giannini, C. Bachmann, C. Luongo, and M. Siccinio

***Abstract*— The Central Solenoid (CS) is at the core of the EU DEMO tokamak, and has a strong impact on the tokamak design and the overall machine size. By ramping its current, the CS generates a change of magnetic flux, which initiates the plasma, and induces and controls the plasma current. In the context of the conceptual design studies for DEMO coordinated by EUROfusion, the Swiss Plasma Center has developed a simple pre-dimensioning methodology, assuming uniform current density in the solenoid winding pack, and considering the use of Nb_3Sn and REBCO. The effects of grading of the superconductor and structural steel are also discussed. Since the CS for the EU DEMO will experience tens of thousands of charge/discharge cycles during its lifetime, mechanical fatigue considerations are taken into account. The proposed methodology has been used for the preliminary design of the CS winding pack, and for a number of parametric analyses in the context of the integrated physics and engineering studies for the EU DEMO machine (identifying the relationship between key performance parameters of the solenoid, such as the generated magnetic flux and the fatigue lifetime).**

***Index Terms*—High-temperature superconductors, Niobium-tin, Solenoids, Superconducting magnets.**

I. Introduction

THE design of the Central Solenoid (CS) has major implications on the overall design, size, and performance of a tokamak. It determines the magnetic flux available to initiate and drive the plasma, the plasma duration, and the lifetime of the machine. Considerations about the structural management of the Lorentz forces in the CS (i.e., reacted by the solenoid winding pack itself or bucked by the Toroidal Field, TF, coils) define the engineering design of the tokamak.

The present baseline design of the European (EU) DEMO tokamak considers a free-standing CS coil in the bore formed by the 16 wedged TF coils, [1]. In the CS, the strongest component of the Lorentz forces pushes radially outward, and, in a free-standing design, it is reacted by the CS winding pack itself. Since the operation of the EU DEMO CS is intrinsically pulsed (it is designed to endure 30,000 plasma cycles during its lifetime), mechanical fatigue of the conductor jackets becomes the main driver in the engineering design of the solenoid. Therefore, it is of utmost importance to include these engineering constraints since the earliest possible stage in the design of the EU DEMO.

This manuscript is divided into two main sections. Section II describes the details and assumptions of the methodology used at the Swiss Plasma Center to pre-dimension the EU DEMO CS. Section III discusses its application in the integrated physics and engineering parametric studies of this project.

II. Methodology

A. Magneto-static Analysis

Unfortunately, there are no closed form expressions for the $\vec{B}$ field generated from a solenoid at any arbitrary point in space. However, the $\vec{B}$ field and vector potential $\vec{A}$ generated by an ideal (infinitesimal cross-section) circular current loop can be expressed in terms of elliptic integrals of the first and second kind and basic mathematical functions [2]–[4]. Thus, the solenoid can be discretized in multiple circular current loops and their elemental contributions can be added up to compute the generated magnetic field and flux at an arbitrary point. This provides great flexibility. For instance, if the solenoid is divided in modules, the current density in each module can be different; the position of the individual loops can be assigned to simulate a uniform current density winding pack (WP) or adjusted to simulate a radially graded WP; and we can also include the contribution of the Poloidal Field (PF) coils of the tokamak.

The only caveat with this approximation is that the expressions for $\vec{B}$ diverge at the infinitesimally thin wire where the current flows. Nevertheless, the expressions for the vector potential $\vec{A}$ do not present discontinuities, and the magnetic flux ψ can be computed from the line integral of $\vec{A}$ over a closed loop of radius R. In an axisymmetric cylindrical geometry:

$$\psi = \oint \vec{A} \cdot d\vec{l} = 2\pi R A_\theta \tag{1}$$

where A_θ is the azimuthal component of $\vec{A}$ in cylindrical coordinates.

Manuscript receipt and acceptance dates will be inserted here. This work has been carried out within the framework of the EUROfusion Consortium, partially funded by the European Union via the Euratom Research and Training Programme (Grant Agreement No 101052200 — EUROfusion). The Swiss contribution to this work has been funded by the Swiss State Secretariat for Education, Research and Innovation (SERI). Views and opinions expressed are however those of the authors only and do not necessarily reflect those of the European Union, the European Commission or SERI. Neither the European Union nor the European Commission nor SERI can be held responsible for them. *(Corresponding author: Xabier Sarasola.)*

X. Sarasola, P. Bruzzone, and K. Sedlak are with the École Polytechnique Fédérale de Lausanne (EPFL), Swiss Plasma Center (SPC), CH-5232 Villigen PSI, Switzerland (e-mail: xabier.sarasola@epfl.ch).

V. Corato, and L. Giannini are with ENEA, Frascati I-00044, Italy.

C. Bachmann, C. Luongo, and M. Siccinio are with the EUROfusion Consortium, D-85748 Garching, Germany.

Color versions of one or more of the figures in this paper are available online at http://ieeexplore.ieee.org.

Digital Object Identifier will be inserted here upon acceptance.

The parametric studies shown in Section III report the magnetic flux at the solenoid outer radius during pre-magnetization, which can be used to estimate the total flux swing provided by the CS.

Even though the approximation of the solenoid by a set of elemental loops provides great flexibility and computes $\vec{B}$ and $\vec{A}$ in a modest amount of time, there are even simpler analytical expressions for the case of a uniform current density cylindrical solenoid with rectangular cross-section and finite height (h). Integrating the individual contributions of the circular current loops [5], the field at the central point of a uniform current density finite solenoid is:

$$B_0 = \frac{\mu_0 j_{eng} h}{2} ln\left\{\frac{\alpha+\sqrt{\alpha^2+\beta^2}}{1+\sqrt{1+\beta^2}}\right\} \quad (2)$$

where μ_0 is the vacuum magnetic permeability in SI units, j_{eng} is the engineering current density in the WP, $\alpha=r_o/r_i$, and $\beta=h/(2r_i)$. Being r_o and r_i respectively the outer and inner radius of the CS WP. B_0 is a good approximation of the maximum field in the WP (B_{max}) for tall solenoids ($\beta>2$), which is the case of the DEMO CS, and the magnetic flux at the CS outer radius can be calculated as:

$$\psi_{CS} = \frac{\pi B_0}{3}(r_i^2 + r_i r_o + r_o^2) \quad (3)$$

Equations (2) and (3) provide a good approximation for the pre-dimensioning studies reported in Section III, because the current density is quite uniform along the height of the solenoid during pre-magnetization, and the radial grading of the WP (in case it is considered) must be limited in order to avoid undesirable radial tension in the solenoid insulation [6].

B. Layout of the Solenoid Winding Pack

The EU DEMO solenoid is assumed to be wound with rectangular Cable-in-Conduit Conductors (CICCs) with steel jackets. The total current in the CS (I_{total}) is distributed uniformly in a certain number of modules (N_{CS}), layers (N_{layers}) and turns per layer ($N_{t,layer}$). The initial assumption considers N_{CS} = 6, N_{layers} = 14, and $N_{t,layer}$ = 40, inspired from ITER [7]–[9]. However, N_{layers} and $N_{t,layer}$ can be reduced (or increased) to set the operating conductor current (I_{op}) within a certain range (typically between 40 and 60 kA). Dedicated studies [10] have shown that this ensures a maximum terminal-to-terminal voltage of each module below 20 kV during normal operation (i.e., plasma breakdown) and at current dump with $\tau = 15$ s. If a lower operating voltage is required, I_{op} can be increased, which for a given I_{total}, results in a marginal gain in generated flux.

The required non-Cu cross-section per turn is computed as $A_{non\text{-}Cu}=I_{op}/(j_{c,non\text{-}Cu}\ cos(\varphi))$, where $j_{c,non-Cu}$ is the non-Cu critical current density, and φ is the lay angle between the strands in the cable and the z-axis along that cable. In these studies, we assume $\cos(\varphi) = 0.98$. The considered $j_{c,non-Cu}$ are the same used in previous studies [11]–[13], and are displayed in Fig. 1. Particularly, the scaling law for Nb_3Sn is that described in [14]. The operating field is the maximum B field in the solenoid (B_{max}), the operating temperature (T_{op}) is 4.75 K and the temperature margin (ΔT_m) for Nb_3Sn is 1.5 K. The assumed operational strain of the Nb_3Sn strands is -0.25% for the react-and-wind (R&W) technology and -0.5% for the wind-and-react (W&R) technology. REBCO tapes operate at 80% of the critical current at 4.75 K.

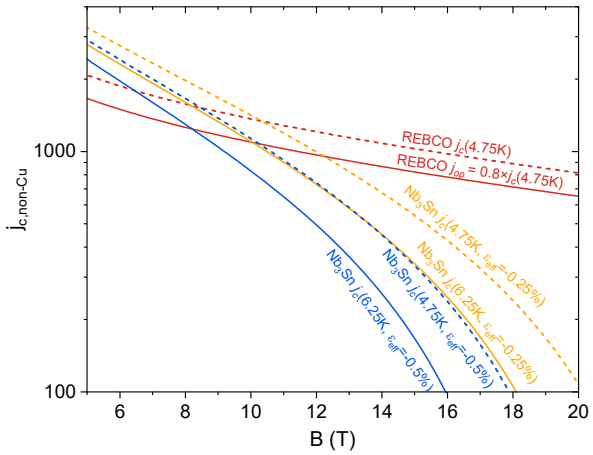

Fig. 1. $j_{c,non-Cu}$ of Nb_3Sn and REBCO as a function of the magnetic field. For Nb_3Sn, T_{op} = 4.75 K, and ΔT_m = 1.5 K. REBCO tapes operate at $j_{op} = 0.8 \times j_{c,non-Cu}(4.75K)$.

The assumed current density in the copper (strands and segregated stabilizer) is $j_{Cu} = 120\ A/mm^2$. This aims at limiting the adiabatic hotspot temperature to 250 K in the strand bundle, based on the enthalpy of the Nb_3Sn and the copper. The overall void fraction (f_{void}) to allow the circulation of supercritical helium amounts to 30% of the total cable space (including bundle and separated cooling channel). Detailed thermal-hydraulic [15] and quench analyses [16] show that these assumptions for j_{Cu} and f_{void} result in reasonably safe designs of the CS WP.

The cross-section of the insulation is calculated using simple geometrical relations and considering the recommendations of EUROfusion for the DEMO magnets: 1 mm around each conductor turn, 2 mm of additional insulation between layers, and 8 mm of ground insulation around each module [14].

For a given geometry of the CS WP, and once the required cross-sections for superconductor, copper, helium and insulation are determined, the remaining space in the WP is assumed to be steel, which represents the largest cross-section in the WP and withstands the Lorentz forces experienced by the solenoid.

C. Mechanical Analysis

The distribution of the hoop (σ_θ) and the radial stress (σ_r) are solved analytically for a uniform current density infinite solenoid [5]. Dedicated Finite Element Models show that those analytical expressions are a good approximation for $\beta>2$ solenoids like the EU DEMO CS.

The expressions in [5] provide σ_θ and σ_r averaged over all the constituents of the WP. In a free-standing CS wound with CICCs, most of the rigidity of the WP is provided by the steel conduits, and thus it is safe to assume that the hoop in the steel (relevant for opening cracks) is $\sigma_{\theta,steel} = \sigma_\theta / f_{steel}$, where f_{steel} is the fraction of steel in the CS WP from Section II.B.

At pre-magnetization, the steel conduits also experience vertical compressive stress, which can be determined from the contribution of the radial B field component. However, the tensile

This article has been accepted for publication in IEEE Transactions on Applied Superconductivity. This is the author's version which has not been fully edited and content may change prior to final publication. Citation information: DOI 10.1109/TASC.2023.3252489

$\sigma_{\theta,steel}$ is the maximum principal stress and drives crack growth. The mechanical analysis focuses on pre-magnetization, since it is associated with the highest magnetic field and largest mechanical stress in the solenoid. At the End-Of-Flattop (EOF) the currents in the central CS modules are fully reversed, and the tensile $\sigma_{\theta,steel}$ is comparable to that experienced during pre-magnetization. Therefore, if the EU DEMO is designed to operate n_p plasma cycles, the design of the central solenoid has to guarantee survival during $2\times n_p$ mechanical cycles.

D. Fatigue Crack Growth Model

Once the cyclic hoop stress in the steel is known, a simple crack growth model based on Linear Elastic Fracture Mechanics (LEFM) is used to estimate the fatigue lifetime. The model uses the Paris law to grow a planar elliptical crack across the thickness of a 2D plate with the width and thickness of the conduit wall, as described in [12], which in turn, follows the assumptions and guidelines of ITER [17] and the EU DEMO [18] for fatigue assessment of mechanical components. The material properties, safety factors, and other assumptions of the crack growth model are also reported in [12]. The criterion for failure considers two cases: crack penetration through the thickness of the conduit wall, and brittle fracture (i.e., the stress intensity factor exceeds the fracture toughness of the conduit material).

III. Parametric Studies

The parametric analyses performed in the context of the integrated physics and engineering studies for the EU DEMO explore a wide range of parameters to pre-dimension the tokamak. In the case of the CS, the parametric spectrum covers:

- a generated B field ranging from 10 to 15 T (for CS designs wound with Nb_3Sn) and 15 to 20 T (for REBCO designs),
- an outer radius of the CS WP ranging from 2.0 (which corresponds approximately to the ITER CS [7]–[9], [19]) and 3.2 m (corresponding to the DEMO baseline 2015 [20]), and
- two possible materials for the conduits: the standard austenitic steel 316LN and the specialty alloy JK2LB used for the ITER CS conduits [8].

The impact of varying the height of the CS WP is very limited for tall ($\beta>2$) solenoids and it remained fixed at 18 m for this parametric exploration.

The target B field determines the total current in the solenoid (Ampere's law). For a given outer radius of the CS WP and a desired pre-magnetization flux ψ_{CS}, the inner radius of the solenoid is also determined making use of (3). This, in turn, defines the current density in the solenoid (j_{eng}) as well as the maximum hoop stress in the steel conduit ($\sigma_{\theta,steel}$ in Section II.C), and ultimately the solenoid fatigue lifetime (Section II.D).

This method allows finding the relationship between key performance parameters of the CS. For instance, Fig. 2 shows how ψ_{CS} varies as a function of the number of plasma cycles for the considered range of outer radii of the CS WP. Thin solenoids provide a larger flux for a given r_o. However, this results in a higher current density in the WP (i.e., lower fraction of steel) and translates into larger mechanical stress in the conduits and lower fatigue lifetime. The figure shows the cases of solenoids generating a field of 13 T, making use of Nb_3Sn R&W as superconductor and JK2LB as jacket material. The case of ITER [7]–[9] is overlaid for reference.

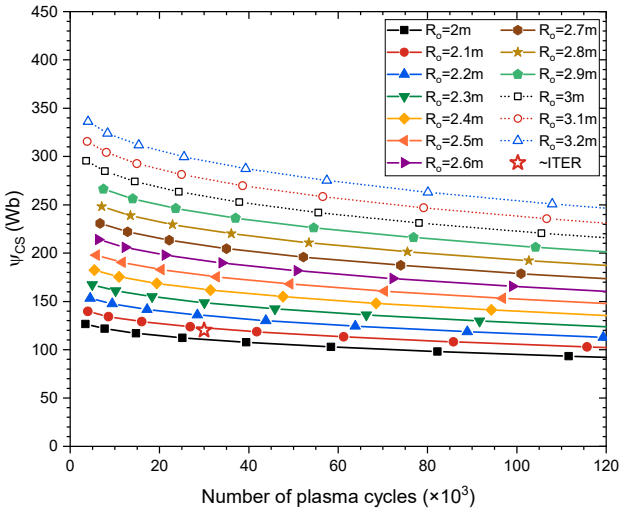

Fig. 2. Generated pre-magnetization flux (ψ_{CS}) as a function of the fatigue lifetime of the solenoid and considering different outer radii of the CS WP. These parametric cases generate a magnetic B field of 13 T, making use of a CS stack with a height h = 18 m. Nb_3Sn R&W (ε_{eff} = -0.25%) is assumed as superconductor and JK2LB as jacket material.

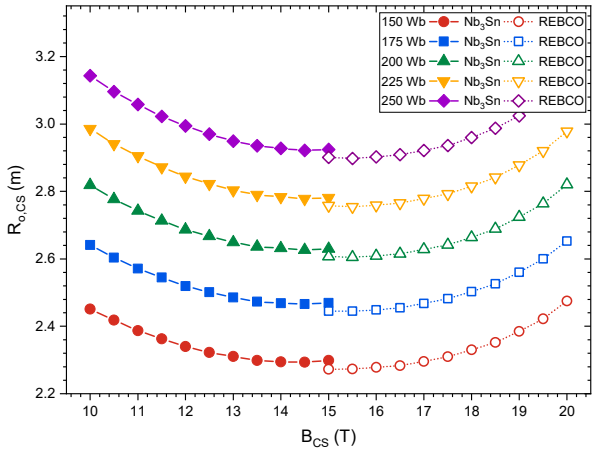

Fig. 3. Outer radius of the solenoid winding pack as a function of the generated magnetic field. Five values of pre-magnetization flux and two superconductors (Nb_3Sn R&W and REBCO) are considered. The jacket material is JK2LB and the fatigue lifetime is limited to 30,000 plasma cycles.

The results in multiple plots like the one shown in Fig. 2 are used to obtain the curves presented in Fig. 3. This figure shows the outer radius of the CS WP required to generate five values of magnetic flux. Nb_3Sn R&W and REBCO are considered as superconductor material, whereas the jacket material is JK2LB and the fatigue lifetime is limited to 30,000 plasma cycles. At low fields, a larger CS is required to generate a certain flux. However, at high fields the larger Lorentz forces involved call for a thicker (i.e., higher steel fraction) solenoid to guarantee the desired fatigue lifetime. For a Nb_3Sn R&W solenoid with

This article has been accepted for publication in IEEE Transactions on Applied Superconductivity. This is the author's version which has not been fully edited and content may change prior to final publication. Citation information: DOI 10.1109/TASC.2023.3252489

JK2LB conduits and the range of flux explored, the most compact CS design is found at a *B* field of ~14.5 T. Fig. 3 also shows that the benefit of using high-temperature superconductor (HTS) is limited because the high current density provided by the REBCO tapes is diluted in the large cross section of steel required to endure tens of thousands of mechanical cycles. Possible means of making a better use of the REBCO tapes can be: to provide radial pre-compression to the CS winding pack (and thus reduce hoop stress in the conduits), to use a double jacket conductor (separating the mechanical and hydraulic functions of the conduits, [21]), or the use of a high mechanical strength stabilizer [22] (also reducing the hoop stress in the conduits).

The use of stainless steel 316LN instead of JK2LB is illustrated in Fig. 4, which shows the size of the CS required to generate the typical pre-magnetization flux of the EU DEMO (250 Wb) while ensuring the required fatigue lifetime (30,000 plasma cycles) as a function of the generated magnetic field. The impact of using SS316LN is somewhat modest (it results in a solenoid with a ~0.2 m larger radius). The lower part of Fig. 4 shows the impact of the solenoid on the machine size. The plasma has been modelled with the reduced transport model PLASMOD [23], [24]. Concerning radial build, the TF coil thickness is estimated as a function of field and current, while other elements such as the breeding blanket thickness, shielding and vacuum vessel thickness are assumed to be constant. All points on the curve have been identified imposing a generated fusion power P_{fus} = 2 GW and a pulse length of 2 h. The pre-magnetization flux for the CS sizing is calculated assuming a constant value for the plasma internal inductance and the Ejima constant, while the value of the loop voltage is provided by PLASMOD. The number of cycles instead is rescaled on the average neutral wall load provided by PLASMOD, so to reach the same neutron fluence as the EU DEMO baseline (70 dpa). The toroidal field is maximized within the space available to ensure radial build consistency. This minimizes the size of the device for the employed assumptions.

Fig. 5 shows the size of the CS considering the number of pulses adapted to the different values of pulse length to match the specified DEMO lifetime fluence associated to an irradiation damage of 70 dpa in the first wall. A constant loop voltage 20 mV is assumed, considering a constant offset of 200 Wb for the ramp-up phase, 10 Wb for breakdown and a spare flux to ensure shape control during ramp-down [25]. At very low pulse length, the number of cycles to obtain the required dpa becomes large and the CS grows because of fatigue. Viceversa, at long pulse length, a high pre-magnetization flux is needed to sustain the discharge, and thus the CS grows again (in spite of the low number of cycles). If JK2LB conduits are used, the curve has a (broad) minimum at ~30 min pulse length. This minimum can be found at ~50 min for stainless steel 316LN conduits.

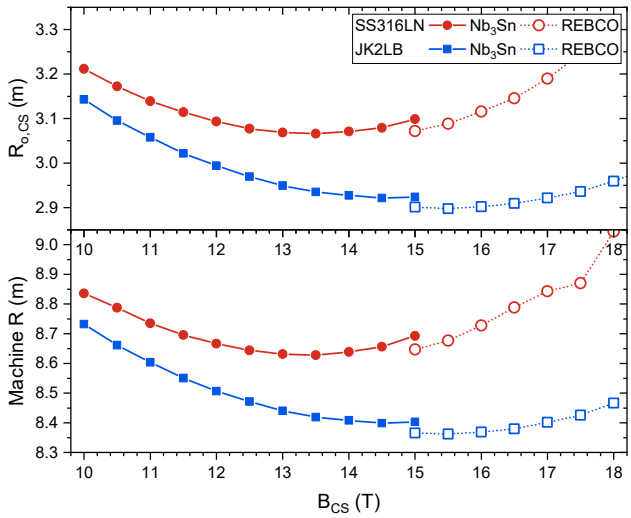

Fig. 4. Outer radius of the solenoid winding pack and machine size as a function of the *B* field generated by the solenoid. All points shown on the plot generate a magnetic flux of 250 Wb and ensure a fatigue lifetime of 30,000 plasma cycles. Two superconductors (Nb_3Sn R&W and REBCO) and two jacket materials (stainless steel 316LN and JK2LB) are considered.

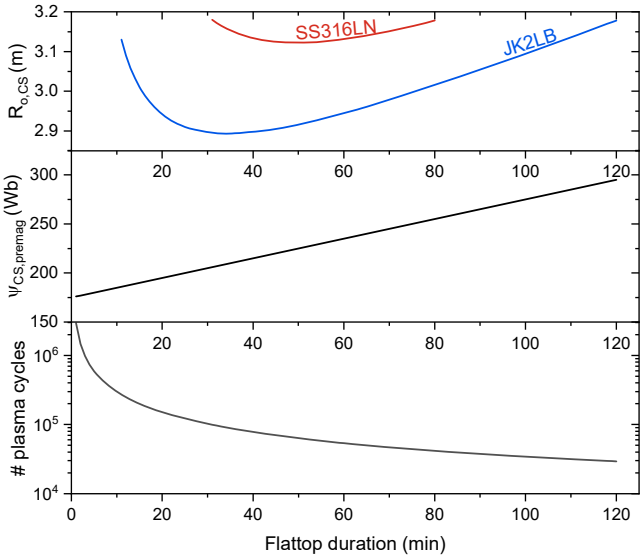

Fig. 5. Outer radius of the solenoid winding pack as a function of the plasma flattop duration for constant dpa and constant loop voltage. Two jacket materials (stainless steel 316LN and JK2LB) are considered. The required pre-magnetization flux and the fatigue lifetime are plotted for convenience, the latter being plotted in semi-logarithmic scale.

IV. Conclusion

A simple methodology is presented to pre-dimension the free-standing Central Solenoid of the EU DEMO. Its use is illustrated in the parametric analyses conducted for the integrated physics and engineering studies of this tokamak, which explores a wide range CS outer radii and *B* fields in order to identify the relationship between key performance parameters of the CS (such as the impact of the number of plasma cycles on the pre-magnetization flux). This methodology has allowed us to determine the *B* field of a solenoid that minimizes the CS outer radius for a target pre-magnetization flux (250 Wb) and fatigue lifetime (30,000 plasma cycles). This optimum can be found at $B_{CS} \approx 13.5$ T for a non-graded Nb_3Sn R&W solenoid with stainless steel 316 LN conduits and it lies at ~14.5 T if JK2LB jackets are used. The described procedure may become a useful tool if incorporated in tokamak reactor systems codes like PROCESS [26].

REFERENCES

[1] V. Corato *et al.*, "The DEMO magnet system – Status and future challenges," *Fusion Engineering and Design*, vol. 174, p. 112971, Jan. 2022, doi: 10.1016/j.fusengdes.2021.112971.

[2] J. D. Jackson, *Classical electrodynamics*, Third ed. New York: J. Wiley & Sons, 1999.

[3] J. C. Simpson, J. E. Lane, C. D. Immer, R. C. Youngquist, and T. Steinrock, "Simple Analytic Expressions for the Magnetic Field of a Circular Current Loop," Jan. 01, 2001. Accessed: Apr. 22, 2022. [Online]. Available: https://ntrs.nasa.gov/citations/20010038494

[4] S. Hampton, R. A. Lane, R. M. Hedlof, R. E. Phillips, and C. A. Ordonez, "Closed-form expressions for the magnetic fields of rectangular and circular finite-length solenoids and current loops," *AIP Advances*, vol. 10, no. 6, p. 065320, Jun. 2020, doi: 10.1063/5.0010982.

[5] M. N. Wilson, *Superconducting Magnets*. Oxford: Clarendon Press, 1987.

[6] N. Mitchell and U. Mszanowski, "Stress analysis of structurally graded long solenoid coils," *IEEE Transactions on Magnetics*, vol. 28, no. 1, pp. 226–229, Jan. 1992, doi: 10.1109/20.119851.

[7] J. H. Schultz *et al.*, "The ITER Central Solenoid," in *21st IEEE/NPS Symposium on Fusion Engineering SOFE 05*, Sep. 2005, pp. 1–4. doi: 10.1109/FUSION.2005.252874.

[8] D. Everitt *et al.*, "ITER Central Solenoid design," in *2013 IEEE 25th Symposium on Fusion Engineering (SOFE)*, Jun. 2013, pp. 1–8. doi: 10.1109/SOFE.2013.6635515.

[9] J. P. Smith *et al.*, "ITER central solenoid module fabrication," in *2013 IEEE 25th Symposium on Fusion Engineering (SOFE)*, Jun. 2013, pp. 1–4. doi: 10.1109/SOFE.2013.6635490.

[10] X. Sarasola, "Exploratory study on the CS coil for the low voltage," 2022. Accessed: May 16, 2022. [Online]. Available: https://idm.euro-fusion.org/?uid=2P8XP7

[11] R. Wesche and X. Sarasola, "Design of the hybrid CS coil based on the 2018 DEMO reference," 2020. [Online]. Available: https://idm.euro-fusion.org/?uid=2NTGP8

[12] X. Sarasola, R. Wesche, I. Ivashov, K. Sedlak, D. Uglietti, and P. Bruzzone, "Progress in the Design of a Hybrid HTS-Nb3Sn-NbTi Central Solenoid for the EU DEMO," *IEEE Transactions on Applied Superconductivity*, vol. 30, no. 4, pp. 1–5, Jun. 2020, doi: 10.1109/TASC.2020.2965066.

[13] R. Wesche *et al.*, "Hybrid HTS-Nb3Sn-NbTi DEMO CS coil design optimized for maximum magnetic flux generation," *Fusion Engineering and Design*, vol. 146, pp. 10–13, Sep. 2019, doi: 10.1016/j.fusengdes.2018.10.027.

[14] "Common operating values for DEMO magnets design for 2016." http://www.euro-fusionscipub.org/archives/eurofusion/common-operating-values-for-demo-magnets-design-for-2016-2 (accessed Apr. 30, 2019).

[15] A. Dembkowska, M. Lewandowska, and X. Sarasola, "Thermal-Hydraulic Analysis of the DEMO CS Coil," *IEEE Transactions on Applied Superconductivity*, vol. 28, no. 4, pp. 1–5, Jun. 2018, doi: 10.1109/TASC.2018.2809425.

[16] A. Dembkowska, M. Lewandowska, X. Sarasola, and K. Sedlak, "Quench analysis of the DEMO CS1 coil," *Cryogenics*, vol. 112, p. 103194, Dec. 2020, doi: 10.1016/j.cryogenics.2020.103194.

[17] C. Jong, "Magnet Structural Design Criteria Part 1: Main Structural Components and Welds," 2012. https://user.iter.org/?uid=2FMHHS

[18] J. Lorenzo, X. Sarasola, and M. Mantsinen, "Fatigue Stress Assessment in Fusion Magnet Components," Nov. 13, 2020. https://idm.euro-fusion.org/?uid=2PBDRG

[19] W. Reiersen, "ITER DDD11-3: CS Coils and Pre-Compression Structure," Nov. 13, 2013. https://user.iter.org/?uid=2NHKHH

[20] R. Ambrosino and R. Albanese, "Reference flat top equilibria for DEMO with aspect ratio 3.1," 2015. Accessed: Feb. 03, 2022. [Online]. Available: https://idm.euro-fusion.org/?uid=2AQ5GP

[21] M. Verrecchia, D. Bessette, N. Mitchell, and Y. Krivchenkov, "ITER-FEAT central solenoid structural analysis and fatigue life assessment," *Fusion Engineering and Design*, vol. 58–59, pp. 141–146, Nov. 2001, doi: 10.1016/S0920-3796(01)00415-X.

[22] G. Celentano *et al.*, "Design of an Industrially Feasible Twisted-Stack HTS Cable-in-Conduit Conductor for Fusion Application," *IEEE Transactions on Applied Superconductivity*, vol. 24, no. 3, pp. 1–5, Jun. 2014, doi: 10.1109/TASC.2013.2287910.

[23] E. Fable, C. Angioni, M. Siccinio, and H. Zohm, "Plasma physics for fusion reactor system codes: Framework and model code," *Fusion Engineering and Design*, vol. 130, pp. 131–136, May 2018, doi: 10.1016/j.fusengdes.2018.03.061.

[24] K. V. Ellis, H. Lux, E. Fable, R. Kembleton, and M. Siccinio, "The next step in systems modelling: The integration of a simple 1D transport and equilibrium solver." [Online]. Available: https://scientific-publications.ukaea.uk/wp-content/uploads/P2.1076.pdf

[25] R. Wenninger *et al.*, "Advances in the physics basis for the European DEMO design," *Nucl. Fusion*, vol. 55, no. 6, p. 063003, Apr. 2015, doi: 10.1088/0029-5515/55/6/063003.

[26] M. Kovari *et al.*, "'PROCESS': A systems code for fusion power plants – Part 2: Engineering," *Fusion Engineering and Design*, vol. 104, pp. 9–20, Mar. 2016, doi: 10.1016/j.fusengdes.2016.01.007.